

Evaluation of thermal properties of PEEK samples made by MEX

SPINA Roberto^{1,2,3,a*} and GURRADO Nicola^{1,b}

¹Dip. di Meccanica, Matematica e Management, Politecnico di Bari, Italy

²Istituto Nazionale di Fisica Nucleare (INFN) - Sezione di Bari, Italy

³Consiglio Nazionale delle Ricerche - Istituto di Fotonica e Nanotecnologie (CNR-IFN), Italy

^aroberto.spina@poliba.it, ^bnicola.gurrado@poliba.it

Keywords: Material Extrusion, PEEK, Thermal Properties

Abstract. The work studies the Polyether ether ketone (PEEK) specimens realized with the material extrusion (MEX) process, evaluating thermal material properties for potential application for polymer heat exchangers. The research investigates the influence of infill density on the thermal properties of PEEK components. A specific instrument measured PEEK specimens' thermal conductivity, thermal diffusivity, and specific heat. The procedure initially required a two-point calibration with references in the investigated ranges, followed by measurement with variable-filled specimens from sparse (20% infill) to full (100% infill). The results indicate that a decrease in the infill value causes a positive reduction in the thermal conductivity and specific heat. In contrast, the diffusivity remains stable with the infill variation.

Introduction

Heat exchangers (HXs) are indispensable in several industrial and engineering applications to eliminate the excessive heat generated during a process or operation by transferring heat between fluids in motion. The HX design results from the complex balance between maximizing the part's surface area and minimizing the pressure drop within the part. A large amount of heat exchange surface per unit of volume characterizes a compact HX. For this reason, maximizing heat transfer by reducing the total volume of the component can lead to a successful design. The combination of topological optimization in the design phase and Additive Manufacturing (AM) in the construction phase improves the expansion of the production space of HXs [1].

Polymer HXs, a particular class among HXs, are a promising alternative to metal HXs for critical applications requiring low weight, low surface energy, antifouling, and anti-corrosion properties. Despite these advantages, polymer HXs are limited by their low inherent thermal conductivity compared to metal HXs, usually two or three orders lower than metals such as stainless steel and aluminum. In heat transfer applications, where the wall thermal resistance has an appreciable impact on the overall thermal resistance, substituting polymers for metals can require significantly more area to achieve the same total heat transfer. The main strategies to reduce the impact of wall thermal resistance are using extremely thin wall thicknesses, lower than <100 μm, or adding a high thermal conductivity filler to the polymer to form a composite [2]. Advanced design topologies can also improve the low thermal conductivity of PHXs. The low conductivity of polymeric materials could be compensated by optimizing geometric parameters, reaching the performances of compact metallic HXs [3]. Heat exchanger geometry is a critical factor in its performance. Conventional manufacturing techniques cannot make these complex geometries. Additive manufacturing (AM) enables the fabrication of complex heat transfer features for next-generation polymer HXs. This is particularly relevant for PHXs due to their low processing temperatures and, thus, cost-effective manufacturing. The fabrication of a physical model allows the design evaluation and then the physical model testing. This would give further data to compare

to the analytical and numerical results gained and further evidence of the design’s practical use for the given application [4].

This work investigates the thermal properties of PEEK specimens realized with the Material Extrusion (MEX) process. PEEK has excellent potential in HXs application due to its chemical resistance and mechanical and thermal properties. For this reason, it is crucial to investigate the influence of infill density on the thermal properties of PEEK components by using an instrumented measuring system to determine the thermal conductivity, thermal diffusivity, and specific heat.

Materials and Methods

Polyether ether ketone (PEEK), a semicrystalline thermoplastic, is among the world’s highest-performing functional materials due to its excellent biocompatibility, chemical resistance, and mechanical and thermal properties, which are retained at high temperatures. 1.75 mm diameter filaments were used for PEEK (naturally unfilled - code KT-820-NT) and PEEK CF (filled with 30% carbon fibers - code KT-820-CF30). The two materials were characterized by a different color, a variable not considered during this analysis [5]. The primary material data supplied by Solvay Group (Bruxelles, Belgium) are reported in Table 1.

The specimens were realized using the FUNMAT HT, a Fused Filament Fabrication (FFF) printer produced by Intamsys Technology Co., Ltd. (Shanghai, China). This printer had a build volume of 260×260×260 mm³. All samples with dimensions 100×10×5 mm³ were printed with a layer height of 200 μm, an infill of 20%, 60%, and 100% with an internal grid pattern, three bottom and three top layers, and three walls (Fig.1). The printer nozzle was 600 μm diameter. Specimens were printed flat on the build platform (XY plane) with a printing speed of 25 mm/s, a nozzle temperature of 410°C, a build plate of 120°C, and a heating chamber of 90°C. Three specimens per time were simultaneously printed, keeping the printing parameters constant after the initial tuning to evaluate the thermal properties, not the AM process.

Table 1: Material data [6]

Physical property	PEEK (KT-820-NT)	PEEK CF (KT-820-CF30)
Density ρ	1.30 [g/cm ³]	1.41 [g/cm ³]
Glass transition temperature T_g	150 [°C]	150 [°C]
Melt temperature T_m	340 [°C]	340 [°C]
Thermal conductivity λ	0.24 [W/m×°C]	0.37 [W/m×°C]
Specific heat capacity c_p	2.15 [kJ/Kg×°C]	1.62 [kJ/Kg×°C]
Tensile Strength σ_R	96 [MPa]	217 [MPa]
Young’s modulus E	3.5 [GPa]	19.7 [GPa]
Elongation at break	20-30 [%]	2 [%]

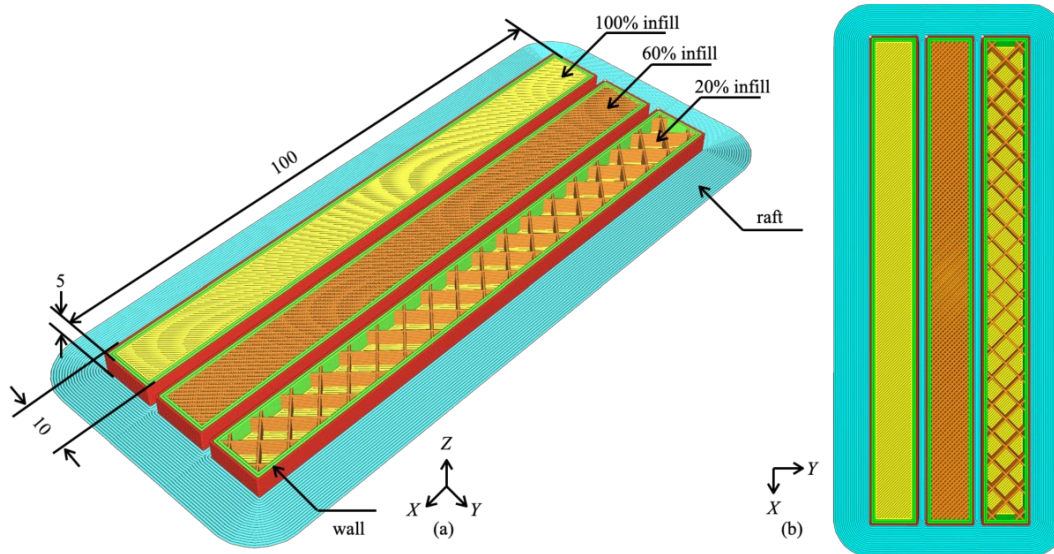


Fig. 1. Specimens in (a) isometric view and (b) top view (all dimensions in mm).

The thermal conductivity of all specimens was then measured using an instrument supplied by Linseis Messgeraete GmbH (Selb, Germany) based on the Transient Hot-Point (THP) method. This instrumentation needed any sample preparation. The THP method estimated the thermal signal's propagation time t through a material sample by applying a short-duration heat pulse to the thermal sensor. Due to the specific layout, the constant electric current flowing through the sensor generated an inhomogeneous temperature profile within the specimens. The THP sensor, an evolution of the transient hot-strip technique, was developed to measure small or anisotropic samples by arranging nickel (laminated version) in a printed circuit foil between two insulating polyimide layers. The sensor, with an overall size of $65 \times 5 \times 0.06 \text{ mm}^3$, was able to measure thermal conductivity in the range of $0.1 \div 2 \text{ W/m} \times \text{K}$ between -150 and 200°C . The bridge was inherently balanced at a uniform temperature, and no nulling was required before running a test. An electric current through the unequally spaced strips established an inhomogeneous temperature profile, resulting in an unbalanced condition. The sensor produced an offset-free output signal of high sensitivity as a measure of the thermal conductivity of the surrounding specimen [7].

The theory behind the hot point sensor was based on a small-point heat source. The thermal conductivity λ and the thermal diffusivity α were determined from a single curve by plotting the temperature rise ΔT on a $t^{1/2}$ time scale and locating the linear part of the curve for long measurement times. λ and α were computed as

$$\lambda = \frac{\phi}{4\pi \times r \times n} \tag{1}$$

$$\alpha = \frac{1}{\pi} \times \left(\frac{n \times r}{m} \right)^2 \tag{2}$$

where ϕ was the sensor heat flow rate, r was the effective radius of the sensor (constant), and n and m were the intercept and the slope of the temperature signal ΔT versus the inverse square of time $t^{1/2}$. The specific heat capacity c_p and the thermal effusivity e were determined using the following equations, give the density ρ :

$$c_p = \frac{\lambda}{\alpha \times \rho} \tag{3}$$

$$e = \frac{\lambda}{\sqrt{\alpha}} = \sqrt{\lambda \times \rho \times c_p} \tag{4}$$

Results and Discussion

Before testing the two PEEK grades, the sensor was calibrated with some standards as reference materials, such as Polymethylmethacrylate (PMMA) and Polyacetal (POM-C), the data of which are reported in [Table 2](#). A two-point calibration was used by re-scaling the sensor output, correcting both slope and offset errors of the sensor response. This calibration was employed because the sensor output was reasonably linear over the measurement range. The PMMA conductivity was near the low end of the measurement range, whereas the POM-C was near the high end.

The thermal conductivities of unfilled and filled PEEK materials were within the range of the reference materials. The tests were conducted at room temperature according to UNI-EN ISO 22007 standard, with a maximum execution time t_{max} of 60 s and a pulse supply current of 50 mA. The calibration procedure allowed the sensor flow rate ϕ correlation with the thermal conductivity λ and diffusivity e for these reference materials, identifying constants from the interpolation of the calibration curve [8].

Table 2: Material data of the reference materials.

Physical property	PMMA	POM-C
Density ρ	1.19 [g/cm ³]	1.41 [g/cm ³]
Glass transition temperature T_g	117 [°C]	-60 [°C]
Melt temperature T_m	- [°C]	166 [°C]
Thermal conductivity λ	0.19 [W/m×°C]	0.39 [W/m×°C]
Specific heat capacity c_p	2.15 [kJ/Kg×°C]	1.40 [kJ/Kg×°C]
Tensile Strength σ_R	77 [MPa]	67 [MPa]
Young's modulus E	3.3 [GPa]	2.8 [GPa]
Elongation at break	5.5 [%]	32 [%]

The test of the unfilled PEEK and filled PEEK specimens with different infill was reported in [Fig.2](#). The infill variable was crucial, as previous research revealed [9]. The temperature rise ΔT rapidly increased in the first time steps, and it became stable after 16 seconds, remaining constant. The maximum time t_{max} was sufficient for reliable results. The maximum temperature variation ΔT_{max} recorded during the test was below 5°C. The initial temperature was equal to the room temperature for studying the air conditioning case. The higher the temperature rise, the lower the infill value. Identical results were identified by plotting the gradient $\Delta T/\Delta t$ vs. $t^{-1/2}$ ([Fig.3](#)), where the $t^{-1/2}$ equal to 0.25 s^{-1/2} corresponded to t of 16 s. Using the inverse square of time $t^{-1/2}$ instead of the logarithm of time $\log(t)$ was functional to represent the graph abscissa between 0 and 1 for t greater than 1 s. The maximum gradient $\Delta T/\Delta t$ slightly changed with the infill value, remaining in the same interval for both materials. The maximum value of the $\Delta T/\Delta t$ was inverse to the infill, pointing out that the same heat flux generated a higher temperature rise.

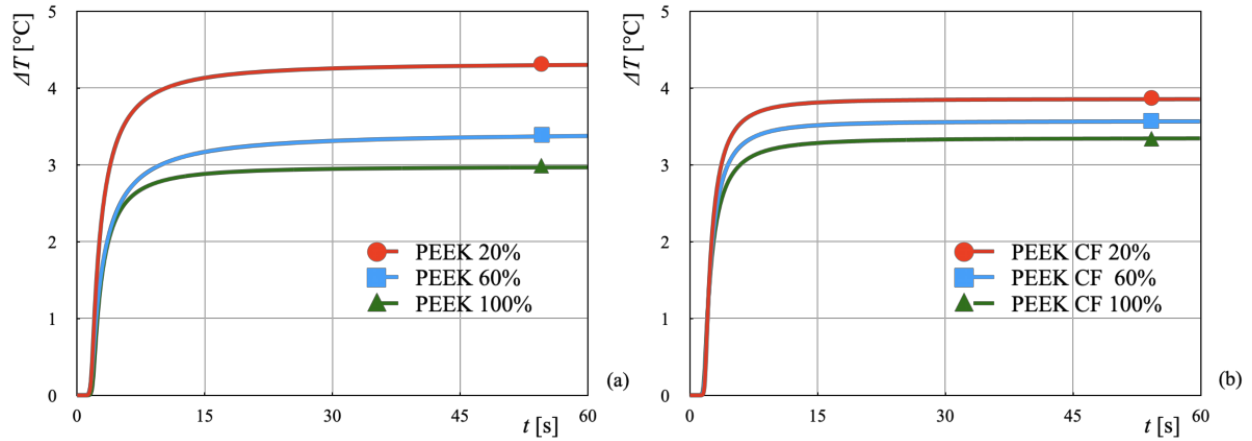


Figure 2. Temperature rise ΔT vs. time t for PEEK (a) and PEEK CF (b) specimens.

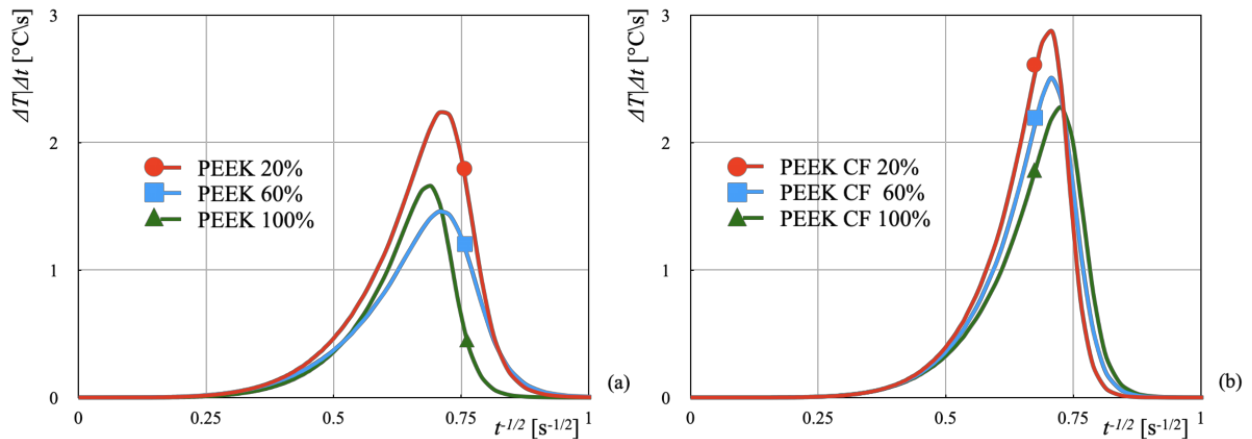


Figure 3. Gradient $\Delta T/\Delta t$ vs. time $t^{1/2}$ for PEEK (a) and PEEK CF (b) specimens.

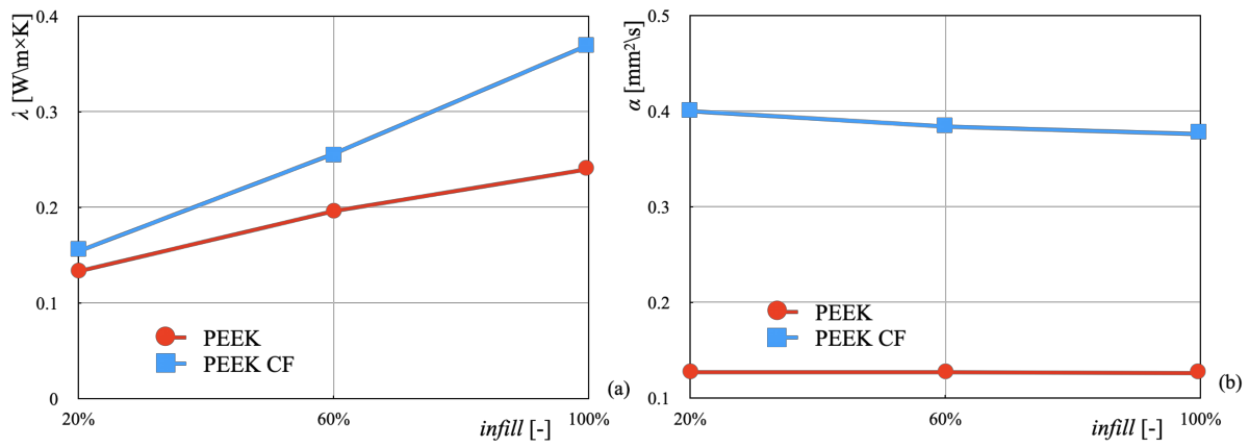


Figure 4. Thermal conductivity λ (a) and diffusivity α (b) vs. infill.

Once the measurement process was analyzed in terms of the THP signal, the following step was the analysis of the thermal properties. Figure 4 reports the variation of the thermal conductivity λ (a) and diffusivity α (b) with infill. A decrease in the infill value caused a positive reduction in the thermal conductivity λ . For the lowest value of the infill, the thermal conductivity was quite the same for both PEEK materials. In contrast, for the highest value of the infill, the contribution of

the carbon fiber fillers was more evident. The behavior of the thermal diffusivity α was different because it remained pretty stable with the infill variation for both materials and different infill.

Figure 5 reports the change of the specific heat c_p (a) and thermal effusivity e (b) with infill. The tendency of the specific heat c_p differed between the two PEEK materials. The unfilled PEEK had a linear correlation with the infill, with a c_p reduction with an infill decrease. The behavior of filled PEEK presented a significant variation with an infill of 60%, remaining stable below this value. For the lowest infill, the specific heat c_p was quite the same, with a small contribution of the carbon fiber. The behavior of the thermal effusivity e also differed in the two PEEK materials. It positively increased with infill in the filled PEEK. In the case of unfilled PEEK, e was relatively stable until the 60% infill and rapidly decreased for lower infill values.

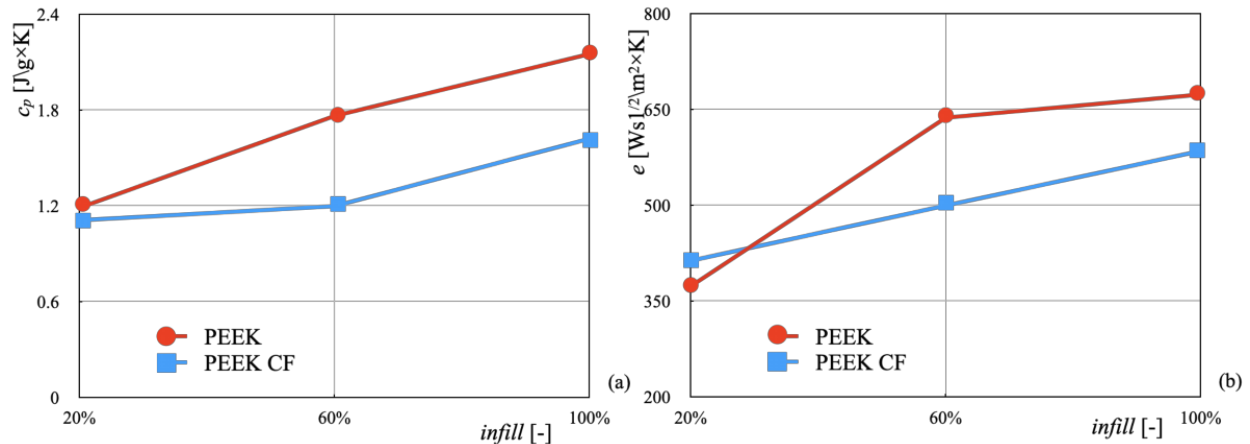


Figure 5. Specific heat c_p (a) and thermal effusivity e (b) vs. infill.

Conclusions

This work investigated the variation of the thermal properties of additively manufactured PEEK with different infill and carbon fiber content. In particular, PEEK specimens were examined using the transient hot point (THP) method after being produced with an additive material extraction (MEX) process with different infill values.

The following conclusions can be drawn from the experimental results. A short time was needed with THP to reach the stationary conditions for the thermal analysis, independently from the material, fiber content, and infill values. The following data analysis pointed out that a decrease in the infill value caused a positive reduction in the thermal conductivity λ . At the same time, effusivity e was not influenced by the infill variation.

To be adopted in polymer exchangers made with MEX, further analysis is required to improve these results to composite materials with high carbon fiber content.

Acknowledgments

The authors wish to thank Prof Luigi Galantucci, Prof Fulvio Lavecchia, and Luigi Morfini of Politecnico di Bari for their suggestions, Claudio Filippo of M. Penati srl and Erika Hahn of Linseis Messgeraete GmbH for the technical support.

The Project was funded under the program Department of Excellence - Law number 232/2016 (Grant No. CUP - D93C23000100001), the National Recovery and Resilience Plan (NRRP), Mission 4 Component 2 Investment 1.3 - Call for tender No. 341 of 15/03/2022 of the Italian Ministry of University and Research (MUR), funded by the European Union – NextGenerationEU, and the RIPARTI funding (assegni di Ricerca per ripartire con le Imprese) of the Apulia Region.

References

- [1] F. Careri et al. Additive manufacturing of heat exchangers in aerospace applications: A review. *Applied Thermal Engineering* 235 (2023) 121387. <https://doi.org/10.1016/j.applthermaleng.2023.121387>
- [2] X. Chen et al. Recent research developments in polymer heat exchangers - A review. *Renewable and Sustainable Energy Reviews* 60 (2016) 1367-1386. <https://doi.org/10.1016/j.rser.2016.03.024>
- [3] B. Ahmadi, S. Bigham. Performance Evaluation of hi-k Lung-inspired 3D-printed Polymer Heat Exchangers. *Applied Thermal Engineering* 204 (2022) 117993. <https://doi.org/10.1016/j.applthermaleng.2021.117993>
- [4] O. Bonner-Hutton et al. Analysis of gyroid heat exchangers for superconducting electric motors. *Materials Today: Proceedings*. in Press. <https://doi.org/10.1016/j.matpr.2023.03.780>
- [5] R. Spina, Performance analysis of colored PLA products with a fused filament fabrication process. *Polymers* 11 (2019) 1984. <https://doi.org/10.3390/polym11121984>
- [6] KetaSpire[®] PEEK Design and Processing Guide. Information on: <https://www.solvay.com/>.
- [7] R. Model, R. Stosch, U. Hammerschmidt. Virtual experiment design for the Transient Hot-Bridge sensor. *International Journal of Thermophysics*, 28 (2007) 1447-1460. <https://doi.org/10.1007/s10765-007-0152-8>
- [8] K.D. Antoniadis et al. Reference Correlations for the Thermal Conductivity of Solid BK7, PMMA, Pyrex 7740, Pyroceram 9606 and SS304. *International Journal of Thermophysics* (2020) 41:98. <https://doi.org/10.1007/s10765-020-02678-9>
- [9] L. Morfini, N. Gurrado, R. Spina. Effect of process parameters on the thermal properties of material extruded AM parts. *Materials Research Proceedings*. 35 (2023) 225- 231. <https://doi.org/10.21741/9781644902714-27>